

INDEPENDENT JOINT CONTROL OF ROBOT MANIPULATORS

Bruno Siciliano

Dipartimento di Informatica e Sistemistica
Università degli Studi di Napoli Federico II
Via Claudio 21, 80125 Napoli, Italy

Abstract

Industrial robot manipulators typically have high gear ratios and are required to move at low operational speed. It is commonly assumed that the nonlinear coupling dynamic terms can be neglected so that conventional linear controllers at each independent joint can be employed. This paper is aimed at presenting independent joint control schemes that are capable to guarantee satisfactory tracking capabilities in spite of disturbance due to dynamic coupling and parameter variations. Three different schemes are analyzed: position feedback, position + velocity feedback, position + velocity + acceleration feedback. The basic idea is to adopt a PI action for the inmost feedback loop, so as to get perfect steady-state disturbance torque rejection. It is shown that the third scheme achieves the best performance in terms of disturbance rejection ratio and recovery time during the transients. Acceleration is reconstructed by means of a suitable state variable filter. Enhanced tracking is obtained by resorting to a linear feedforward action.

1. Introduction

The problem of motion control of an articulated mechanical system is to determine the time history of the generalized forces (forces or torques) to be developed at the actuators of the controlled axes of motion so as to guarantee the execution of the commanded task while satisfying given transient and steady-state requirements.

Several methodologies can be employed for controlling this kind of system. The technique followed as well as the way it is implemented may have a significant influence on the system performance and then on the possible range of applications. For instance, the need for trajectory tracking control may lead to hardware/software implementations which differ from those allowing a point-to-point control where only reaching of the final position, and not of the actual trajectory followed, is of concern.

On the other hand, the mechanical design has an influence on the kind of control scheme utilized. In other terms, a mechatronic trade-off has to be sought between the mechanical structure of the system and the architecture of the control unit.

As a classical paradigm to illustrate the effects of mechanical design on the motion control problem, consider a robot manipulator for which the driving system has an effect on the type of control strategy used. If the manipulator is actuated with DC

motors and gear train drives with high gear ratios, it typically has a nearly decoupled dynamics which simplifies the control action. The price to pay, however, is the occurrence of joint friction, elasticity and backlash that may limit system performance. On the other hand, a manipulator actuated with direct drives eliminates the above drawbacks but usually requires a more complex control action to account for those terms in the model playing a relevant role at considerable operational speeds and accelerations.

It is known that, in the case of direct-drive manipulators, the dynamic terms play a significant role for high-speed motions [1]. A large number of model-based control schemes were proposed [2,3], including adaptive control algorithms [4,5,6]. More recently, however, it was demonstrated that also for industrial robot manipulators with high gear ratios dynamic compensation yields significant reduction of tracking errors [7,8]. Nevertheless, we still believe that decentralized control schemes of industrial type can perform well in a wide number of applications.

The present work is based on the results in [9,10,11] and proposes *independent joint control* schemes which are shown to guarantee satisfactory tracking capabilities in spite of inertia and load variations. Three different schemes are proposed: position feedback, position + velocity feedback, position + velocity + acceleration feedback. The basic idea is to adopt a PI action for the inmost feedback loop, so as to get perfect steady-state rejection of constant disturbance torques. It is shown that the third scheme achieves the best performance in terms of disturbance rejection ratio and recovery time during the transients. The problem of lack of direct acceleration measurements is solved by using a state variable filter to reconstruct them. Further, it is shown how linear feedforward compensation confers enhanced tracking capabilities to the schemes in case of good model accuracy.

2. Independent Joint Control

It is well known that the dynamic model of an n -degree-of-freedom robot manipulator in free space is given by

$$B(q)\ddot{q} + C(q, \dot{q})\dot{q} + g(q) = \tau \quad (1)$$

where q is the $(n \times 1)$ vector of joint variables, B is the $(n \times n)$ positive definite symmetric inertia matrix, $C\dot{q}$ is the $(n \times 1)$ vector of Coriolis and centrifugal forces, g is the $(n \times 1)$ vector of gravitational forces, and τ is the $(n \times 1)$ vector of joint driving forces.

To control the motion of the manipulator means to determine the forces τ that allow the execution of a motion $q(t)$ such that

$$q(t) = q_d(t)$$

as closely as possible, where $q_d(t)$ indicates the vector of reference joint variables.

Focusing on the case of gear-driven robots, the joint forces are provided by the actuators via kinematic transmissions that perform a motion transformation from the motors to the links. If q_m is the $(n \times 1)$ vector of actuator displacements, the following relation is obtained

$$K_r q = q_m \quad (2)$$

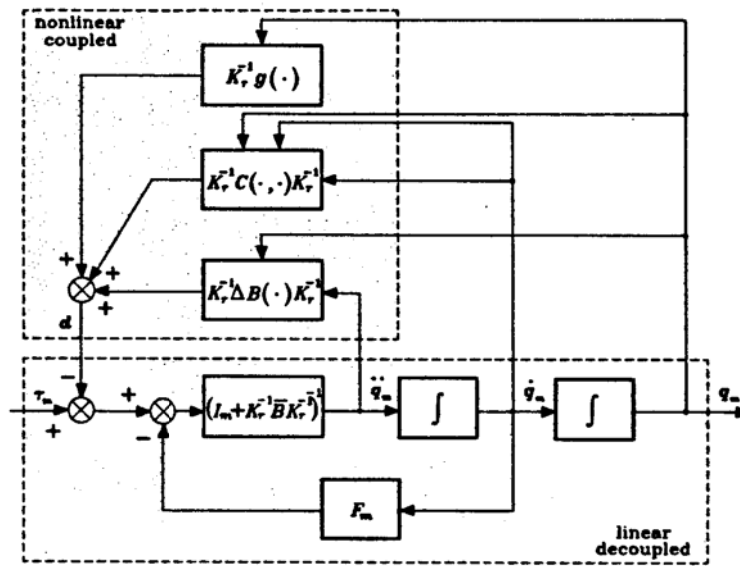


Figure 1: Block scheme of the dynamics of a gear-driven industrial robot manipulator

where K_r is an $(n \times n)$ diagonal matrix whose elements are usually much greater than unity.

Due to the presence of gear reductions, the vector of actuator driving forces τ_m is given by

$$\tau_m = I_m \ddot{q}_m + F_m \dot{q}_m + K_r^{-1} \tau \quad (3)$$

where I_m and F_m are diagonal matrices whose elements are the inertias and viscous friction coefficients of the gear reduction motors, and $K_r^{-1} \tau$ is the vector of required joint torques resulting at the actuator axes.

At this point, observing that the diagonal elements of $B(q)$ contain inertia moments that do not depend on the joint configuration and configuration-dependent terms of sinusoidal functions, the inertia matrix can be decomposed as

$$B(q) = \bar{B} + \Delta B(q) \quad (4)$$

where \bar{B} is a diagonal matrix whose constant elements represent the average values of joint inertias. Plugging (2-4) into (1) gives

$$\tau_m = (I_m + K_r^{-1} \bar{B} K_r^{-1}) \ddot{q}_m + F_m \dot{q}_m + \tau_{NL} \quad (5)$$

where

$$\tau_{NL} = K_r^{-1} \Delta B(q) K_r^{-1} \ddot{q}_m + K_r^{-1} C(q, \dot{q}) K_r^{-1} \dot{q}_m + K_r^{-1} g(q). \quad (6)$$

As evidenced by the block scheme of Fig. 1, the system of the manipulator structure and the mechanical part of the gear reductions is actually composed of two subsystems; one with τ_m as input and q_m as output, the other with $q_m, \dot{q}_m, \ddot{q}_m$ as input

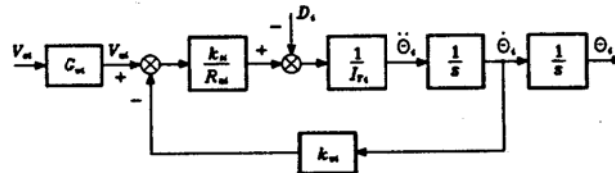


Figure 2: Block scheme of the dynamics of an individual manipulator joint

and τ_{NL} as output. The former is *linear* and *decoupled*; each component of τ_m affects the corresponding component of q_m . The latter is *nonlinear* and *coupled*, since it accounts for all those nonlinear and interacting contributions stemming from the joint coupled dynamics.

On the basis of the above scheme, τ_{NL} can be regarded as a vector of *disturbance forces* for the joint servos. This corresponds to a *decentralized* structure of the controller, i.e. an *independent joint control* can be designed.

3. Disturbance Rejection

It is desired to find a control structure that allows satisfactory tracking of the output reference variable with suitable reduction of disturbance effects; hence, the two goals of the design are *disturbance rejection* and *trajectory tracking*. Consider first the problem of disturbance rejection.

The system to control is the servo of the i th joint of the manipulator. If a voltage-controlled motor is assumed, the servo has the block scheme of Fig. 2 which is logically derived from the scheme in Fig. 1. In detail, the i th motor is characterized by the average inertia

$$I_{Ti} = I_{mi} + k_{ri}^{-2} \bar{b}_{ii},$$

the resistance of the armature circuit R_{ai} (the inductance has been neglected), and the torque and voltage constants k_{ti} and k_{vi} , respectively. Further, G_{vi} indicates the voltage gain of the power amplifier that usually precedes the motor. Consequently, the input to the system is not the armature voltage v_{ai} , but the input voltage v_{ci} of the amplifier. The scheme of Fig. 2 evidences the presence of the disturbance input d_i that turns out to be the i th component of the torque vector τ_{NL} in (6), i.e.

$$d_i = \sum_{k=1}^n k_{ri}^{-1} k_{rk}^{-1} b_{ik} \ddot{\theta}_k - k_{ri}^{-2} \bar{b}_{ii} \ddot{\theta}_i + \sum_{k=1}^n k_{ri}^{-1} k_{rk}^{-1} c_{ik} \dot{\theta}_k + k_{ri}^{-1} g_i \quad (7)$$

where \bar{b}_{ii} is the average, constant value of inertia at the i th joint, and k_{ri} is the gear ratio of the i th joint. Notice that in the scheme of Fig. 2, the viscous friction coefficient F_{mi} has been assumed negligible with respect to the equivalent electrical friction coefficient $k_{vi} k_{ti} / R_{ai}$. Moreover, the following positions are made:

$$k_{mi} = \frac{1}{k_{vi}} \quad T_{mi} = \frac{R_{ai} I_{Ti}}{k_{vi} k_{ti}}$$

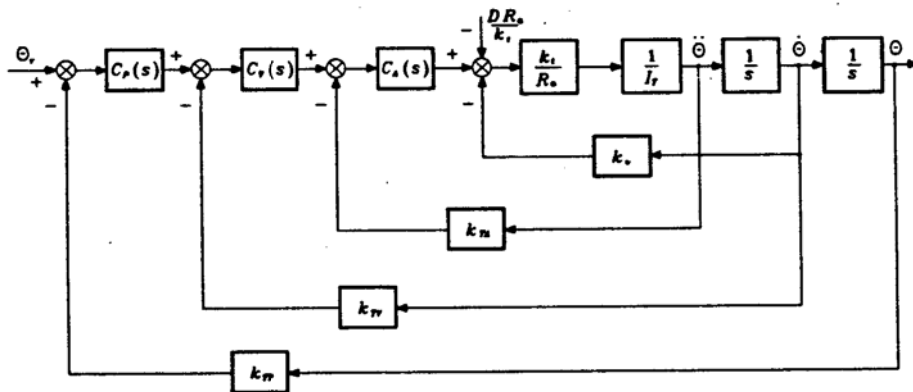


Figure 3: Block scheme of the position + velocity + acceleration feedback control system

where k_{mi} and T_{mi} are respectively the gain and time constants of the motor; G_{vi} is considered to be included in the controller gain. Hence, the motor is described by the voltage to position transfer function—dropping, from now on, the subscript i for notation compactness—

$$M(s) = \frac{k_m}{s(1 + sT_m)} \tag{8}$$

An effective rejection of the disturbance d is ensured by:

- a large value of the power amplifier gain,
- an integral action in the controller so that the effect of the gravitational component on the output θ is annihilated at steady-state.

This clearly suggests the use of a *PI* action for the controller whose transfer function is

$$C(s) = K_c \frac{1 + sT_c}{s};$$

this yields zero error at steady-state for a step disturbance, and the presence of the real zero in $s = -1/T_c$ offers a stabilizing function.

Besides the closure of a position feedback loop, the most general solution is obtained by closing inner feedback loops on the velocity and acceleration. This leads to the scheme in Fig. 3, where $C_P(s)$, $C_V(s)$, $C_A(s)$ represent respectively the *position*, *velocity*, *acceleration* controllers, k_{TP} , k_{TV} , k_{TA} are the relative transducer constants, and the amplifier gain constant has been embedded in the gain constant of the inner controller. Notice also that the disturbance torque D has been appropriately transformed into a disturbance voltage by the factor R_a/k_t .

In the following, the three particular solutions deriving from the general scheme of Fig. 3 are presented; at this stage, the eventual issue arising from measurement of physical variables is not considered yet.

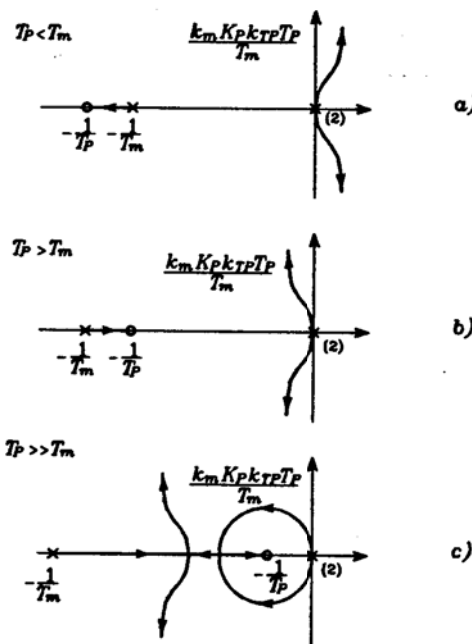


Figure 4: Root loci for the position feedback scheme

3.1. Position Feedback

In this case:

$$C_P(s) = K_P \frac{1 + sT_P}{s}, \quad C_V(s) = 1, \quad C_A(s) = 1$$

$$k_{TV} = k_{TA} = 0.$$

Root locus analysis can be performed as the gain of the position loop varies. Three situations are evidenced for the closed-loop poles (Fig. 4). The stability of the closed-loop feedback system imposes some constraints on the choice of the parameters of the PI regulator: If $T_P < T_m$, the system is inherently unstable (Fig. 4a). Then, it must be $T_P > T_m$ (Fig. 4b). As T_P increases, however, the absolute value of the real part of the two roots of the locus tending towards the asymptotes increases too, and the system has faster time response. Hence, it is convenient to render $T_P \gg T_m$ (Fig. 4c). In any case, the real part of the couples of dominant poles cannot be less than $-T_m/2$.

The closed-loop input/output transfer function is

$$\frac{\Theta(s)}{\Theta_i(s)} = \frac{\frac{1}{k_{TP}}}{1 + \frac{s^2(1 + sT_m)}{k_m K_P k_{TP}(1 + sT_P)}}, \quad (9)$$

while the closed-loop disturbance/output transfer function is

$$\frac{\Theta(s)}{D(s)} = -\frac{\frac{sR_d}{k_i K_P k_{TP}(1+sT_P)}}{1 + \frac{s^2(1+sT_m)}{k_m K_P k_{TP}(1+sT_P)}} \quad (10)$$

It can be recognized that the term $K_P k_{TP}$ is the reduction factor imposed by the feedback gain on the amplitude of the output due to the disturbance; then, the quantity

$$X_R = K_P k_{TP} \quad (11)$$

can be interpreted as the disturbance rejection factor. However, it is not appropriate to increase K_P too much, because small damping ratios would result leading to unacceptable oscillations of the output. Further, for large values of K_P , the third root on the real axis is almost cancelled by the neighbouring zero. On the other hand, it can be noticed in (10) that also the closed-loop zero in $s = -1/T_P$ is cancelled by the pole at denominator; thus, the closed-loop pole close to the zero is not cancelled anymore and then determines the dynamics of the disturbance, which is quite slow. A characterization of the recovery time to the disturbance is then given by the time constant

$$T_R = T_P. \quad (12)$$

3.2. Position + Velocity Feedback

In this case:

$$C_P(s) = K_P, \quad C_V(s) = K_V \frac{1+sT_V}{s}, \quad C_A(s) = 1$$

$$k_{TA} = 0.$$

Root locus analysis can be performed as the gain of the velocity loop varies. The most convenient choice is to utilize the zero of the regulator in $s = -1/T_V$ to cancel the effects of the real pole of the motor in $s = -1/T_m$. By setting

$$T_V = T_m,$$

the poles of the closed-loop system move on the root locus as the gain of the velocity loop varies (Fig. 5). The increase of K_P allows to move the roots towards regions of the left-half complex plane characterized by large values of the real part, if an opportune choice of K_V is made.

The closed-loop input/output transfer function is

$$\frac{\Theta(s)}{\Theta_i(s)} = \frac{\frac{1}{k_{TP}}}{1 + \frac{sk_{TV}}{K_P k_{TP}} + \frac{s^2}{k_m K_P k_{TP} K_V}}, \quad (13)$$

which can be compared with the typical transfer function of a second-order system

$$W(s) = \frac{\frac{1}{k_{TP}}}{1 + \frac{2\zeta s}{\omega_n} + \frac{s^2}{\omega_n^2}} \quad (14)$$

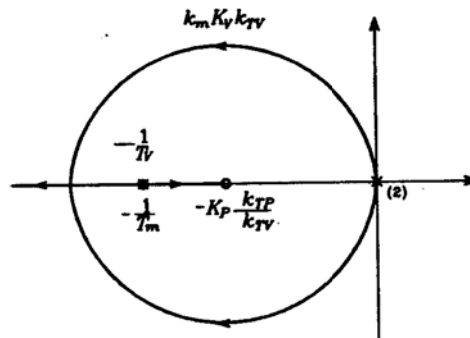


Figure 5: Root locus for the position + velocity feedback scheme

It can be recognized that, with a suitable choice of the gains, it is possible to get all the values of natural frequency ω_n and damping ratio ζ . Hence, if ω_n and ζ are given as design requirements, the following relations can be established:

$$K_V k_{TV} = \frac{2\zeta\omega_n}{k_m} \quad (15)$$

$$K_P k_{TP} K_V = \frac{\omega_n^2}{k_m} \quad (16)$$

Once K_V and k_{TV} have been chosen to satisfy (15), the values of K_P and k_{TP} are obtained from (16).

Further, the closed-loop disturbance/output transfer function is

$$\frac{\Theta(s)}{D(s)} = -\frac{sR_n}{k_i K_P k_{TP} K_V (1 + sT_V)} \cdot \frac{1}{1 + \frac{s k_{TV}}{K_P k_{TP}} + \frac{s^2}{k_m K_P k_{TP} K_V}}, \quad (17)$$

which shows that the disturbance rejection factor is

$$X_R = K_P k_{TP} K_V \quad (18)$$

and is fixed, once K_P and K_V have been chosen via (15,16). Concerning the disturbance dynamics, the presence of a zero in the origin introduced by the PI and of three poles having real parts $-1/T_V$, $-\zeta\omega_n$, $-\zeta\omega_n$ should be noticed. Hence, in this case, an estimate of the disturbance recovery time is given by the time constant

$$T_R = \max\left\{T_m, \frac{1}{\zeta\omega_n}\right\}, \quad (19)$$

which reveals an improvement with respect to the previous case in (11), since $T_m \ll T_P$.

3.3. Position + Velocity + Acceleration Feedback

In this case:

$$C_P(s) = K_P, \quad C_V(s) = K_V, \quad C_A(s) = K_A \frac{1 + sT_A}{s}$$

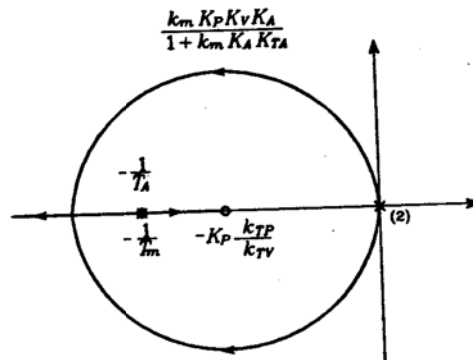


Figure 6: Root locus for the position + velocity + acceleration feedback scheme

Differently from the previous case, the presence of the acceleration feedback does not allow to define the motor transfer function as in (8). It is necessary, in fact, to perform some handy manipulation of the block scheme in Fig. 3, so as to report the acceleration loop in parallel to the velocity loop of the motor. It can be shown that, also in this case, an opportune cancellation can be performed by setting

$$T_A = T_m$$

or

$$k_m K_A k_{TA} T_A \gg T_m \quad k_m K_A k_{TA} \gg 1.$$

The two solutions are essentially the same, as far as the dynamic features of the control system are concerned. In both cases, in fact, the closed-loop poles are constrained on the root locus in Fig. 6. This turns out to be analogous to the one in Fig. 5, having assimilated the system to a second-order one.

The closed-loop input/output transfer function is

$$\frac{\Theta(s)}{\Theta_i(s)} = \frac{\frac{1}{k_{TP}}}{1 + \frac{sk_{TV}}{K_P k_{TP}} + \frac{s^2(1 + k_m K_A k_{TA})}{k_m K_P k_{TP} K_V K_A}} \quad (20)$$

Moreover, the closed-loop disturbance/output transfer function is

$$\frac{\Theta(s)}{D(s)} = -\frac{\frac{sR_d}{k_i K_P k_{TP} K_V K_A (1 + sT_A)}}{1 + \frac{sk_{TV}}{K_P k_{TP}} + \frac{s^2(1 + k_m K_A k_{TA})}{k_m K_P k_{TP} K_V K_A}} \quad (21)$$

The resulting disturbance rejection factor and recovery time are respectively given by

$$X_R = K_P k_{TP} K_V K_A \quad (22)$$

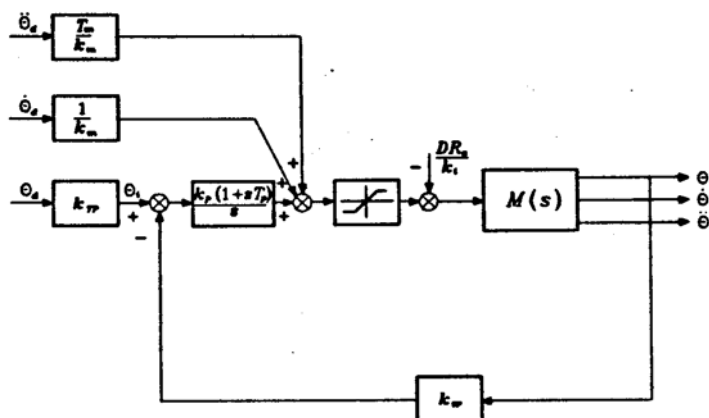


Figure 8: Block scheme of position feedback control with decentralized feedforward compensation

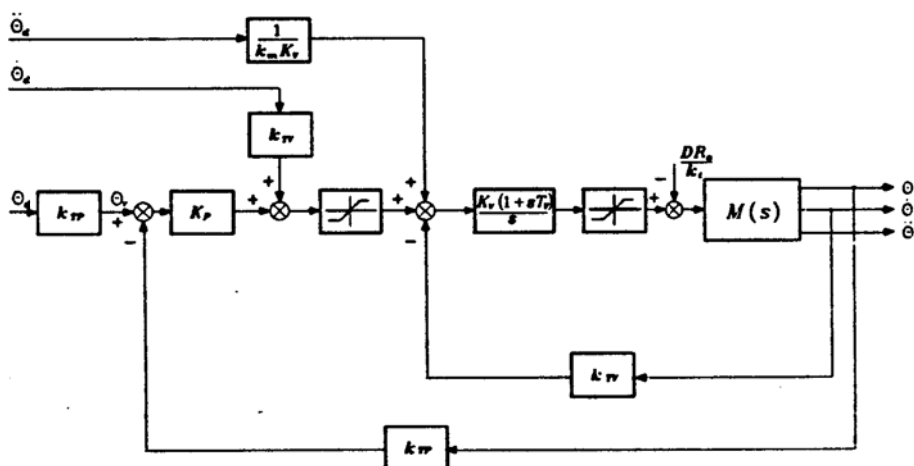


Figure 9: Block scheme of position + velocity feedback control with decentralized feedforward compensation

position trajectories with high values of speed and acceleration, the tracking capabilities of the scheme in Fig. 3 may become quite poor.

A computationally cheap remedy to the above inconvenient can be obtained via the well-known technique of feedforward cancellation of the plant dynamics. In particular, it is quite straightforward to recognize that if the reference inputs to the three control

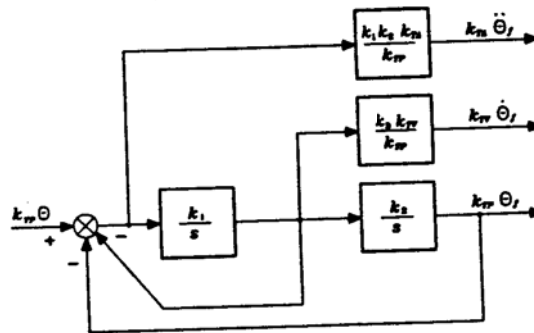


Figure 7: Block scheme of the state variable filter

and

$$T_R = \max\left\{T_A, \frac{1}{\zeta\omega_n}\right\} \quad (23)$$

where T_A can be made less than T_m .

With reference to the transfer function in (14), the following relations can be established for design purposes:

$$\frac{2K_P k_{TP}}{k_{TV}} = \frac{\omega_n}{\zeta} \quad (24)$$

$$1 + k_m K_A k_{TA} = \frac{k_m X_R}{\omega_n^2} \quad (25)$$

$$K_P k_{TP} K_V K_A = X_R \quad (26)$$

Once K_P , k_{TP} and k_{TV} have been chosen to satisfy (24), K_A and k_{TA} are chosen to satisfy (25), and then K_V is obtained from (26). Therefore, with respect to the previous case, now the acceleration feedback remarkably allows not only to achieve any desired dynamic behaviour, but also to prescribe the disturbance rejection factor.

In deriving the above three control schemes, the issue of measurement of feedback variables was not considered explicitly. With reference to the typical position control servos that are implemented in industrial practice, there is no problem to measure position and velocity, while a direct measurement of acceleration in general either is not available or is too expensive to get. Therefore, for the general scheme of Fig. 3 with position + velocity + acceleration feedback, an indirect measure is to be obtained, that is the acceleration measurement is reconstructed from the position measurement by means of a state variable filter (Fig. 7). The filter is characterized by a natural frequency $\omega_{nf} = \sqrt{k_1 k_2}$ and by a damping ratio $\zeta_f = (1/2)\sqrt{k_1/k_2}$. Choosing the filter bandwidth to be larger than the joint servo bandwidth—at least a decade off to the right—the effects due to measurement lags between θ_f and θ are not appreciable, and then it is feasible to take the filter outputs as the quantities to feed back.

4. Trajectory Tracking

The above schemes have been derived according to the purpose of achieving good disturbance rejection. When the joint control servos are required to track reference

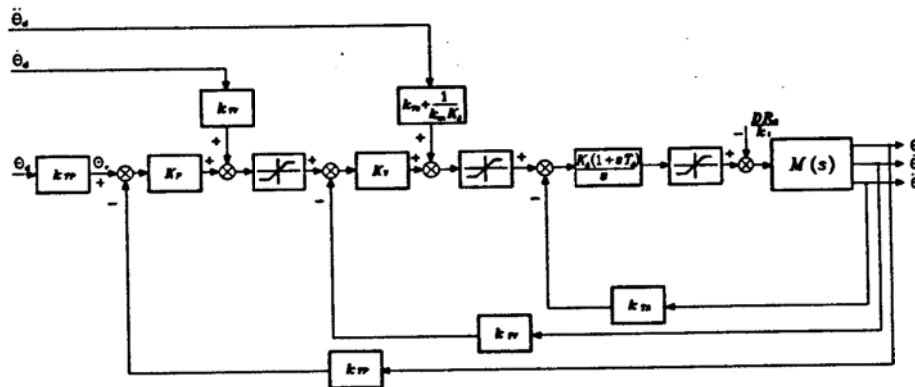


Figure 10: Block scheme of position + velocity + acceleration feedback control with decentralized feedforward compensation

structures analyzed in the previous section are modified respectively into

$$\theta_r = \left(k_{TP} + \frac{s^2(1+sT_m)}{k_m K_P(1+sT_P)} \right) \theta_d \quad (27)$$

$$\theta_r = \left(k_{TP} + \frac{sk_{TV}}{K_P} + \frac{s^2}{k_m K_P K_V} \right) \theta_d \quad (28)$$

$$\theta_r = \left(k_{TP} + \frac{sk_{TV}}{K_P} + \frac{(1+k_m K_A k_{TA})s^2}{k_m K_P K_V K_A} \right) \theta_d, \quad (29)$$

perfect tracking of the desired joint position trajectory is achieved. Incidentally, computing derivatives of the desired trajectory $\theta_d(t)$ is not a problem, once that is known analytically. The tracking control schemes resulting from simple manipulation of Eqs. (27,28,29) are reported respectively in Figs. 8,9,10, where $M(s)$ indicates the voltage-to-position motor transfer function in (8).

All the solutions allow perfect tracking of the input trajectory within the range of validity and linearity of the employed models. Deviations from the ideal values cause a performance degradation that must be analyzed case by case. It is interesting to notice that, as the number of nested feedback loops increases, less knowledge of system model is required to perform feedforward compensation. In fact, T_m and k_m are required to close a position loop, only k_m is required for the position + velocity loops, and k_m again—but with reduced weight—for the position + velocity + acceleration loops.

The schemes of Figs. 8–10 reveal also the presence of saturation blocks. These are to be intended as intentional nonlinearities whose function is that to limit relevant physical quantities during the transients; the greater the number of feedback loops, the greater the number of quantities that can be limited (velocity, acceleration and motor voltage). To this purpose, notice that trajectory tracking is lost when any of the above quantities saturates.

After simple block reduction on the above schemes, it is possible to determine equivalent control structures that utilize position feedback only and regulators with standard

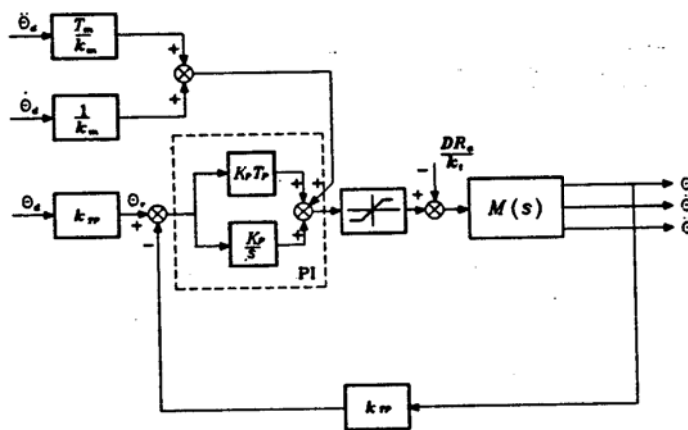


Figure 11: Equivalent control scheme of PI type

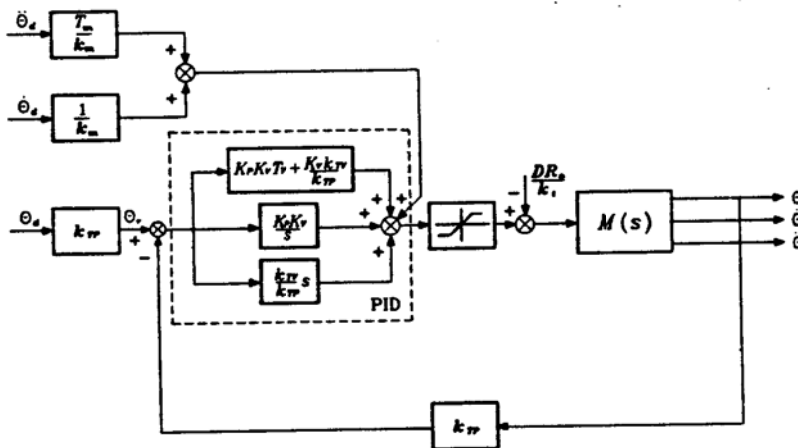


Figure 12: Equivalent control scheme of PID type

dynamic actions. It should be emphasized that the two solutions are equivalent in terms of disturbance rejection and trajectory tracking. However, setting of regulator parameters is less straightforward and the elimination of inner feedback loops prevents the possibility of setting saturations on velocity and/or acceleration. The control structures equivalent to those of Figs. 8,9,10 are illustrated in Figs. 11,12,13. respectively; control actions of PI, PID, PIDD² type are evidenced which are equivalent to the control schemes of position, position + velocity, position + velocity + acceleration type, respectively.

with different sampling rates demonstrated improved performance of the scheme with acceleration feedback over the conventional PID scheme and comparable performance with that obtained with a model-based control scheme.

Acknowledgement

This work was supported by CNR under contract n. 92.01064.PF67.

References

- [1] P.K. Khosla and T. Kanade, "Experimental evaluation of nonlinear feedback and feedforward control schemes for manipulators," *Int. J. of Robotics Research*, vol. 7, no. 1, pp. 18-28, 1988.
- [2] J.J. Craig, *Introduction to Robotics: Mechanics and Control*, 2nd Ed., Addison Wesley, Reading, MA, 1989.
- [3] M.W. Spong and M. Vidyasagar, *Robot Dynamics and Control*, John Wiley & Sons, New York, 1989.
- [4] A. Balestrino, G. De Maria, and L. Sciavicco, "An adaptive model following control for robotic manipulators," *ASME J. of Dynamic Systems, Measurements, and Control*, vol. 105, pp. 143-151, 1983.
- [5] J.-J.E. Slotine and W. Li, "On the adaptive control of robot manipulators," *Int. J. of Robotics Research*, vol. 6, no. 3, pp. 49-59, 1987.
- [6] R. Ortega and M.W. Spong, "Adaptive motion control of rigid robots: A tutorial," *Automatica*, vol. 25, pp. 877-888, 1989.
- [7] M.B. Leahy Jr. and G.N. Saridis, "Compensation of industrial manipulator dynamics," *Int. J. of Robotics Research*, vol. 8, no. 4, pp. 73-84, 1989.
- [8] P. Chiacchio, L. Sciavicco, and B. Siciliano, "The potential of model-based control algorithms for improving industrial robot tracking performance," *Proc. IEEE Int. Workshop on Intelligent Motion Control*, Istanbul, TR, pp. 831-836, 1990.
- [9] P. Chiacchio, L. Sciavicco, and B. Siciliano, "Practical design of independent joint controllers for industrial robot manipulators," *Proc. 1992 American Control Conf.*, Chicago, IL, pp. 1239-1240, 1992.
- [10] P. Chiacchio, F. Pierrot, and B. Siciliano, "Experimenting acceleration feedback loop for robot control," *Proc. 2nd European Control Conference*, Groningen, NL, pp. 565-569, 1993.
- [11] P. Chiacchio, F. Pierrot, L. Sciavicco, and B. Siciliano, "Robust design of independent joint controllers with experimentation on a high-speed parallel robot," *IEEE Trans. on Industrial Electronics*, vol. 40, no. 4, 1993.